Dual jet-mixing reactor for fully continuous synthesis of core@shell Au@Ag nanocomposites

Authors: Pinaki Ranadive,[1] Faiz Khan,[1] Jessica O. Winter,[1,2,*] and Nicholas Brunelli[1,*]

Author address: [1]The Ohio State University, William G. Lowrie Department of Chemical and Biomolecular Engineering, 151 W. Woodruff Ave., Columbus, OH 43210; [2]The Ohio State University, Department of Biomedical Engineering, Columbus, OH 43210

***Corresponding authors:** winter.63@osu.edu; brunelli.2@osu.edu; Twitter: OSUChemEProfBru

Supplemental information

S1. Synthesis of Au NP cores for two step batch synthesis

A batch reactor is used to produce Au NPs cores for core@shell Au@Ag NP synthesis. The sample is characterized using UV-vis (Figure S1a) and TEM (Figure S1b).

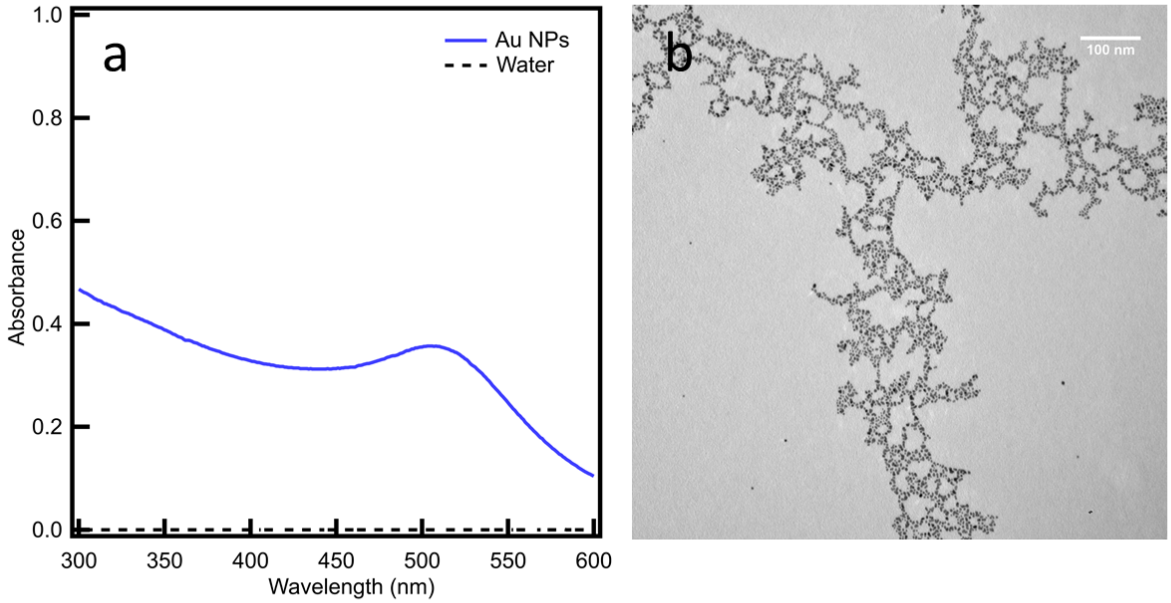

Figure S1a. UV-vis spectrum, and **b.** representative TEM image of Au NPs synthesized in batch with 0.27 mM $HAuCl_4$ and 2.40 mM $NaBH_4$ as given in literature.[1]

S2. Batch studies of Au NP synthesis without stabilizing ligand

The effect of $NaBH_4$ concentration on Au NP properties is investigated through studies in batch and using the JMR. The concentration of $NaBH_4$ is varied from 0.60 mM to 2.40 mM in

separate batch and JMR syntheses while maintaining a constant $HAuCl_4$ concentration of 0.27 mM. For the batch method, the UV-vis spectra obtained for each sample are shown in Figure S2 (compared to JMR at similar conditions) and S3 (results for batch experiments with different $NaBH_4$ concentrations). All spectra indicate maximum absorbance at wavelengths between 510-530 nm, consistent with the surface plasmon resonance band of Au NPs.[1–3] Peaks for JMR synthesized particles were red-shifted compared to those for batch synthesis, indicating slightly larger particle size. With increasing $NaBH_4$ concentration in batch, the UV-vis peak in the region of 510 nm appears to blue-shift toward smaller wavelengths – associated with decreased particle size – and reaches a relatively steady maximum value after a concentration of 0.90 mM.

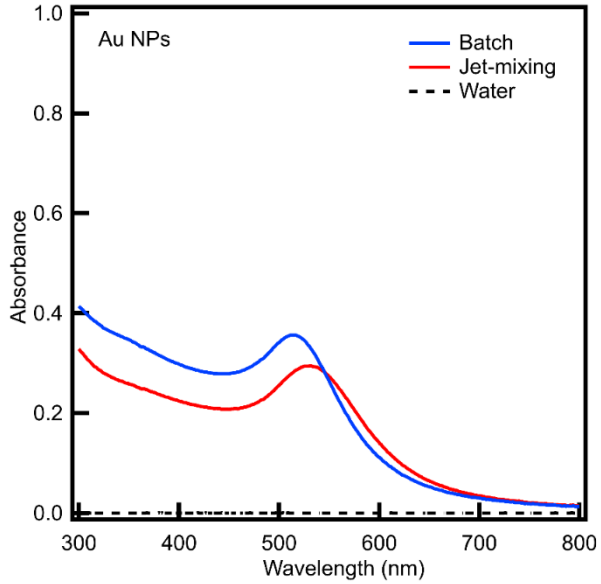

Figure S2. UV-vis spectra of batch-synthesized *(blue)* and jet-mixing synthesized *(red)* Au NPs. Au NP synthesis in both processes is conducted using 0.9 mM $NaBH_4$ and 0.27 mM $HAuCl_4$. The batch synthesis is conducted at 200 RPM. The main line and jet line flowrates in the single jet-mixer are maintained at 48 mL/h.

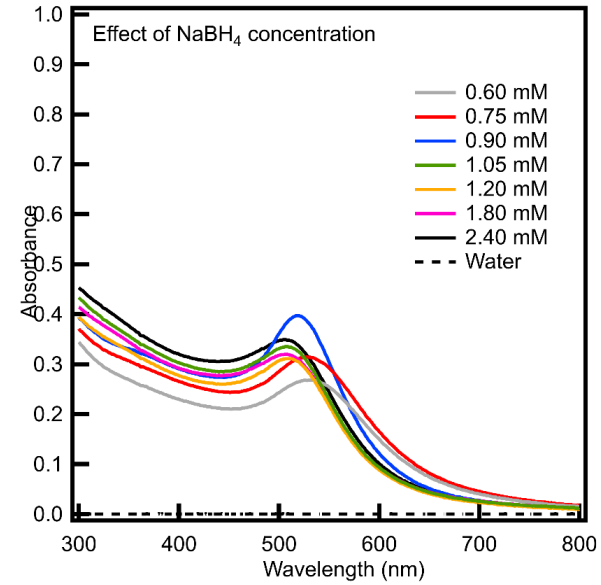

Figure S3. UV-vis spectra of Au NPs synthesized with varying concentrations of $NaBH_4$ and 0.27 mM $HAuCl_4$ in the absence of a stabilizing agent. Equal volumes of $HAuCl_4$ and $NaBH_4$ solutions are added to a batch stirring at 200 RPM to synthesize the Au NPs. Analysis is conducted 10 minutes after synthesis. The maximum absorbance obtained is used for yield calculation.

This is corroborated by DLS data. As the $NaBH_4$ concentration increases, the particle size calculated from DLS data is observed to decrease from 8 nm to 4 nm, as shown in Table S1. DLS results indicate a minimum particle size emerges at a concentration of 1.05 mM. This observation is consistent with nucleation theory and previous work.[1,4,5] An increase in $NaBH_4$ concentration results in an increased rate of nucleation, leading to a burst of small nuclei formation and consequently, reducing the availability of precursors for growth of existing nuclei. The result is high $NaBH_4$ concentration produces a narrow particle size distribution with small average NP size.

Table S1. Effect of $NaBH_4$ concentration on Au NP size and yield synthesized in batch. The $HAuCl_4$ concentration is maintained constant in all syntheses at 0.27 mM. Two batch synthesis are conducted for each $NaBH_4$ concentration with their average properties reported.

[$NaBH_4$] (mM)	Particle size[a] (nm)	Yield (%)[b]
0.60	8 ± 1	73 ± 10
0.75	9 ± 1	80 ± 6
0.90	9 ± 1	92 ± 3
1.05	6 ± 1	99 ± 2
1.20	4 ± 1	96 ± 6
1.80	4 ± 1	93 ± 5
2.40	4 ± 1	105 ± 6

[a] Determined using DLS; [b] Calculated from the particle size and the UV-vis absorption.

The maximum absorbance obtained from the UV-vis spectra and the particle size obtained though DLS is used to calculate the reaction yield (see supplemental information S4). Presented in Table S1 are the average values for two runs for the hydrodynamic particle size obtained through DLS and the yield. The synthesis yield increases with increased $NaBH_4$ concentration, as is expected since the rate of reduction increases with the $NaBH_4$ concentration. At concentrations above 0.90 mM, the upper limit of Au NP nears 100%, suggesting the complete reduction of $HAuCl_4$. Hence, the smallest $NaBH_4$ concentration at which high Au NP yield is obtained is 0.90 mM. It is possible that a $NaBH_4$ concentration of 1.05 mM may be optimal, but the concentration of 0.9 mM is used for further testing to establish the proof-of-concept and reduce the chance of NaBH4 residual entering the downstream JMR. The UV-vis spectrum for batch-synthesized Au NPs with 0.90 mM $NaBH_4$ is shown in Figure S2. The Au NPs synthesized with 0.90 mM $NaBH_4$ are also analyzed by TEM to confirm the particle size. A representative TEM image is shown in Figure S4. Analysis of over 150 particles using ImageJ results in a mean Feret length of 7.7 nm with a positive standard deviation of 7.5 nm and a negative standard deviation of 3.8 nm. The polydispersity index is calculated to be 0.70. The size distribution obtained is similar to the size obtained through DLS (9±1 nm). It should be noted, however, that NP sizes obtained from DLS and TEM vary significantly between replicates as a result of the lack of a capping ligand and should be used with caution.

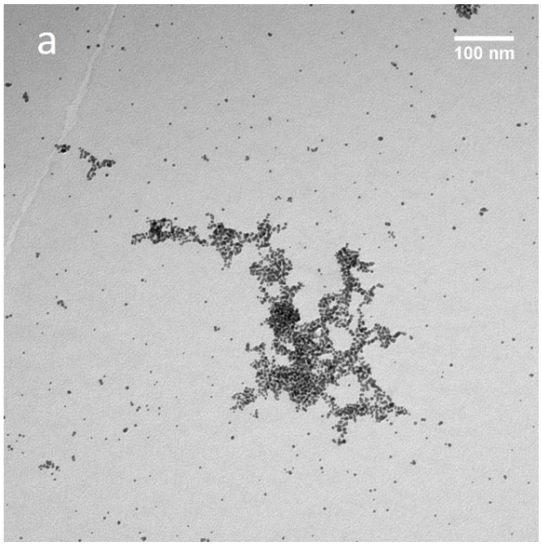

Figure S4. TEM images of Au NPs synthesized in batch with 0.90 mM $NaBH_4$ and 0.27 mM $HAuCl_4$ in absence of stabilizing ligand. The batch synthesis is conducted at 200 RPM.

S3. Comparison between batch and jet-mixing synthesized Au NPs

The size of uncapped Au NPs is analyzed by DLS and TEM for both batch and JM. The comparison is shown in Table S2.

Table S2. Comparison between the particle sizes obtained for batch and JM-synthesized Au NPs. No capping agent has been used in the syntheses. Over 100 particles are analyzed to determine the TEM size distribution. The following synthesis conditions are used: 0.27 mM $HAuCl_4$ and 0.9 mM $NaBH_4$. The main line and jet line flowrates in the single jet-mixer are maintained at 48 mL/h.

Average particle size (nm)	Batch Au NPs	JM Au NPs
DLS (nm)	2.9 ± 0.4	6.4 ± 0.9
TEM (nm)	3.1 ± 1.1	3.4 ± 1.1

It is observed that the size of Au NPs obtained using JM is comparable to that obtained from batch when analyzed through TEM, suggesting that the jet-mixing process preserves Au NP properties obtained from the batch process. The size obtained through DLS is comparable to that obtained through TEM for the batch-synthesized Au NPs, while it is slightly larger for JM-synthesized Au NPs compared to the TEM size. This difference may be attributed to post-synthetic aggregation in the absence of a capping agent prior to analysis.

S4. Au NP yield calculation

The yield is determined by calculating the concentration of Au atoms (C_{Au}). This is obtained from the concentration of Au NPs (C_{AuNP}) determined by applying Beer-Lambert's law (Equation 1).

$$A = \varepsilon_{Au} * C_{AuNP} * L \quad (1)$$

where the absorbance of Au NPs (A) is obtained from UV-visible spectroscopy (UV-vis) analysis; the path length for UV-vis analysis (L) is 1 cm; and the extinction coefficient (ε_{Au}) is derived from literature for citrate-capped Au NPs.[6] The reported values for ε_{Au} at corresponding citrate-capped Au NP sizes (d_{Au}) are extrapolated to derive a linear relationship. The relationship obtained between the extinction coefficient for Au NPs and Au NP size (in nm) is shown in equation 2 (R^2 = 0.995).

$$\ln(\varepsilon_{Au}) = 3.3225 * \ln(d_{AuNP}) + 10.766 \quad (2)$$

Calculations for Au NPs synthesized in batch with 0.9 mM $NaBH_4$ are shown as an example. The particle size through dynamic light scattering analysis for this synthesis is 9±1 nm (d_{AuNP} = 9 nm), resulting in $\varepsilon_{Au} = 7.02 * 10^7\ M^{-1}cm^{-1}$. The absorbance ($A$) obtained at the maximum absorbance wavelength of 506 nm is 0.397. The concentration of Au NPs calculated is therefore:

$$C_{AuNP} = 5.66 * 10^{-9}\ M \quad (3)$$

The average number of Au atoms per nanoparticle (N) is calculated using the known size of the Au NP (d_{AuNP}) and equations 4 through 9.

$$Average\ size\ of\ 1\ NP\ (d_{AuNP}) = 9\ nm \quad (4)$$

$$Volume\ of\ 1\ NP = \frac{\pi * d_{AuNP}^3}{6} = 3.82 * 10^{-25}\ m^3 \quad (5)$$

$$Density\ of\ Au = 19300\ \frac{kg}{m^3} \quad (6)$$

$$Mass\ of\ 1\ NP = Volume * density = 7.37 * 10^{-21}\ kg \quad (7)$$

$$Molar\ mass\ of\ Au = 196.97\frac{g}{mol} \quad (8)$$

$$N = \frac{Mass\ of\ 1\ NP * N_A * 1000}{Molar\ mass\ of\ Au} \approx 22{,}523 \quad (9)$$

Further, N is used to obtain C_{Au}, as shown in equation 10.

$$C_{Au} = C_{AuNP} * N = 1.27 * 10^{-4}\ M = 0.127\ mM \quad (10)$$

The initial concentration of $HAuCl_4$ post-mixing of the reactant solutions ($C_{initial}$ = 0.13 mM) is used to calculate the process yield, as shown in equation 11.

$$Yield = \frac{C_{Au}}{C_{initial}} * 100 \quad (11)$$

For Au NPs synthesized in batch with 0.9 mM $NaBH_4$, the yield is hence calculated to be 95%. Two syntheses are performed, and the average yield calculated from them is reported in Table 1.

S5. Au@Ag NP seeded synthesis

S.5.1. Order of addition of reagents

The order of addition of components for synthesizing Au@Ag NPs is established through initial batch studies. Au NPs prepared in a batch reactor using $HAuCl_4$ as the Au source are further separately capped by Ag through injecting $AgNO_3$ and $NaBH_4$. First, $NaBH_4$ is rapidly injected into a solution containing Au NPs and $AgNO_3$. This leads to the immediate formation of a cloudy, grey precipitate (Batch 1) for which the UV-vis spectrum is shown in Figure 5a. It is observed that the spectrum has a peak around 250 nm. It is hypothesized that the peak may be attributed to AgCl NPs formed in the Au NP + $AgNO_3$ solution that reduce to metallic silver on injection and form

the precipitate. A solution of $AgNO_3$ is mixed with NaCl to form AgCl NPs, for which the HUV-vis spectrum is also shown in Figure 5a. The spectra are close, suggesting the presence of AgCl.

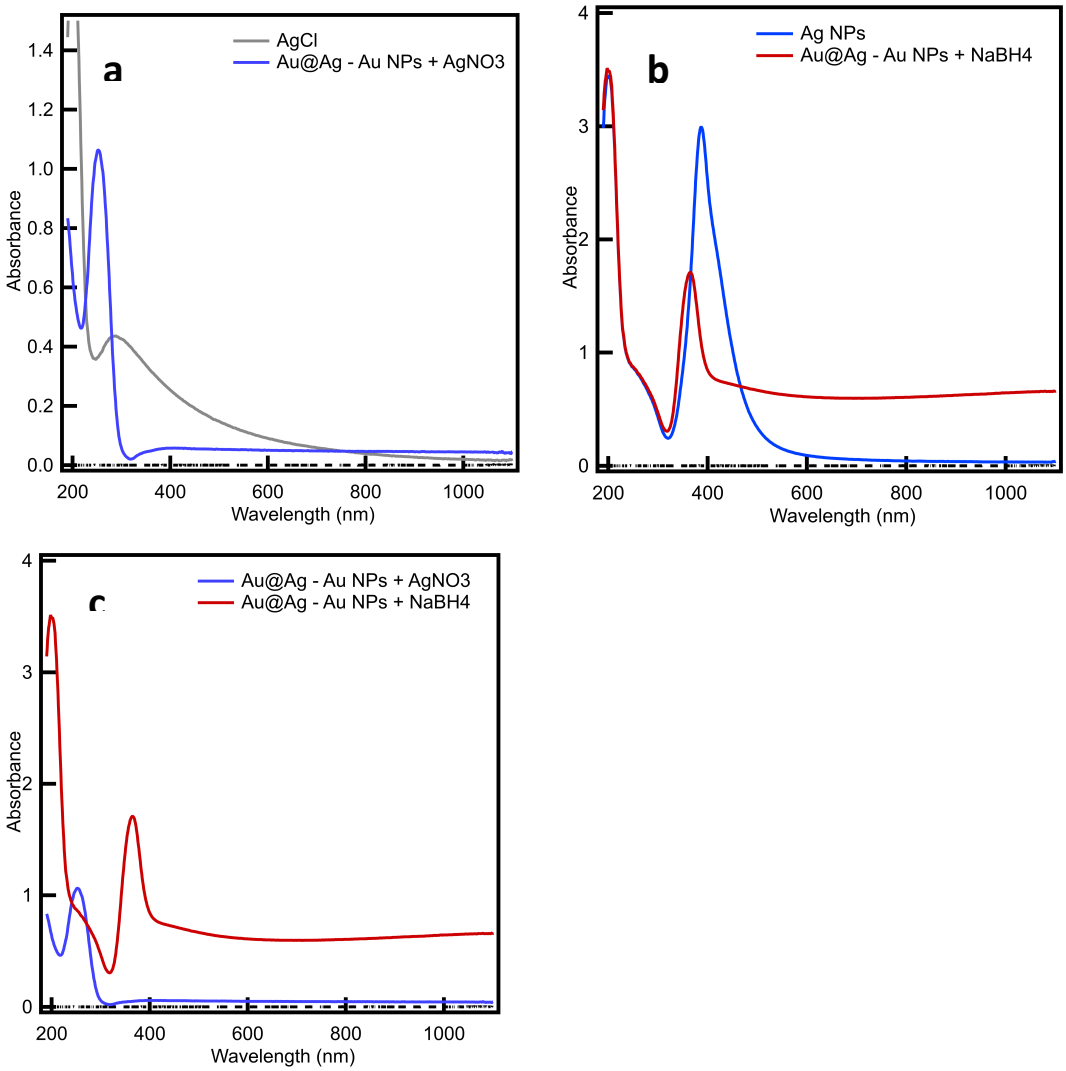

Figure S5. UV-vis spectra obtained by analyzing seeded Au@Ag NP batches synthesized to investigate the effect of order of addition of reagents: (a) Batch 1 (Au NPs + $AgNO_3$ with $NaBH_4$ addition), compared against a spectrum from AgCl NPs; (b) Batch 2 (Au NPs + $NaBH_4$ with $AgNO_3$ addition), compared against Ag NPs synthesized with same reagent solutions without adding Au NPs; (c) Comparison of Batches 1 and 2.

Next, the order of reagent addition is interchanged. $AgNO_3$ is rapidly injected into a solution of Au NPs + $NaBH_4$ (Batch 2). A yellow solution suggests that Ag NPs are formed, and no cloudiness or precipitation is seen. The UV-vis spectrum from this solution is compared to the initial Au@Ag NP solution (Batch 1) in Figure 5b. A strong peak around 400 nm is observed in Batch 2, suggesting the presence of nano-silver. The peak around 250 nm previously associated with AgCl

formation is not observed. Further, the leftover $AgNO_3$ and $NaBH_4$ starting solutions prepared for the Batch 2 synthesis are mixed to form Ag NPs as a control. The comparison of the UV-vis spectra of the Ag NPs and Batch 2 is shown in Fig 5c. The identical nature of the two spectra up to 400 nm further corroborates that this range may correspond to residual Ag NP starting reagents and not to AgCl. Hence, AgCl is concluded to be absent from Batch 2.

These observations are used to adapt the batch synthesis procedure to include the injection of $AgNO_3$ into a solution of Au NPs and the reducing agent. This order of addition of reagents is also further extended to design the dual jet mixing process.

S5.2. Batch studies for Au@Ag NP seeded synthesis

A batch process is investigated for encapsulating the Au seeds by an Ag shell. Au NPs pre-synthesized in batch are used as seeds for selective Ag capping through the reduction of $AgNO_3$ by the mild reducing agent ascorbic acid (AA). The goal is to identify batch synthesis conditions for seeded Au@Ag NPs that favor heterogeneous nucleation of Ag on Au NPs. Specifically, the kinetics of four potential sub-processes are important: (1) heterogeneous nucleation of Ag on Au through $AgNO_3$ reduction by AA; (2) homogeneous nucleation of Ag NPs through reduction of $AgNO_3$ by AA; (3) heterogeneous nucleation of Ag on Au through $AgNO_3$ reduction by residual $NaBH_4$ in solution from Au NP synthesis; and (4) homogeneous nucleation of Ag NPs through reduction of $AgNO_3$ by $NaBH_4$. First, homogenous Ag NP synthesis via AA reduction is investigated. In the absence of Au NPs, $AgNO_3$ and AA solutions are mixed in a batch reactor.[7] Without Au NPs, Ag NP formation is not apparent as the UV-vis spectra lacks a prominent peak at 400 nm (Figure S6a). This observation indicates that homogeneous nucleation of Ag through reduction by AA does not occur at the concentrations investigated.

The Au NPs used in this process are synthesized with 0.9 mM $NaBH_4$, which has yields approaching 100%. Thus, we do not anticipate significant residual $NaBH_4$ to be present in the reaction mixture. This hypothesis is confirmed through a seeded batch Au@Ag NP synthesis. Specifically, Au NPs synthesized using $NaBH_4$ (0.9 mM) are added to an $AgNO_3$ solution (0.06 mM). A UV-vis spectrum of the resulting solution is taken and shown in Figure S6b. A peak around 500 nm that suggests Au NP presence is observed; however, the absence of a peak around 400 nm suggests that Ag NPs are not formed. It is expected that residual $NaBH_4$ in the Au NP solution, if any, would lead to homogeneous nucleation of Ag NPs on contacting with $AgNO_3$. As this is not observed from the UV-vis spectrum, it is concluded that there is no residual $NaBH_4$ remaining post Au NP synthesis.

Hence, sub-processes (2), (3), and (4) are concluded as unlikely based on the above studies. Accordingly, it is anticipated that heterogeneous nucleation of Ag on Au NPs is the most likely out of the remaining three sub-processes.

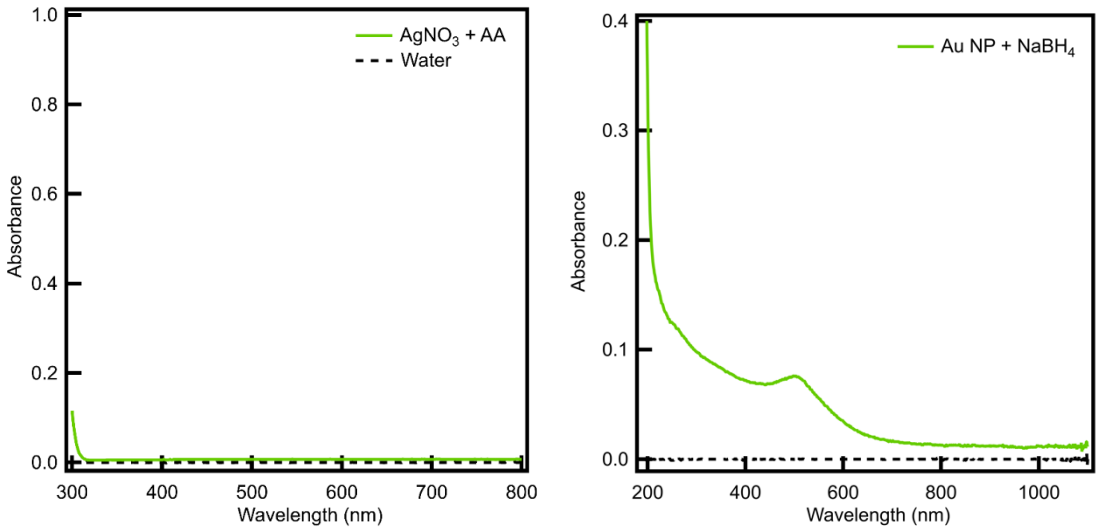

Figure S6a. UV-vis spectrum obtained by analyzing a mixture of $AgNO_3$ solution (0.06 mM, 5 mL) and ascorbic acid solution (2 mM, 4.5 mL) in a batch reactor stirring at 200 RPM. **b.** UV-vis spectrum obtained by analyzing a mixture of AgNO3 solution (0.6 mM) and Au NPs synthesized in batch using $NaBH_4$ (0.9 mM).

Heterogeneous nucleation caused by AA depends on the level of supersaturation that can be related to the rate of Ag^{+1} to Ag^0 formation by reduction.[4] Hence, an increase in AA concentration at a constant Au-to-Ag precursor molar ratio is hypothesized to increase the rate of heterogeneous Ag nucleation. The effect of AA concentration on Au@Ag NP seeded synthesis is investigated by varying the AA concentration from 0.5 mM to 16 mM in separate batch syntheses while maintaining the $AgNO_3$ concentration (0.062 mM) and Au NP volume % in the product (5%) constant. The products from all batches are analyzed through UV-vis spectra, as shown in Figure S7.

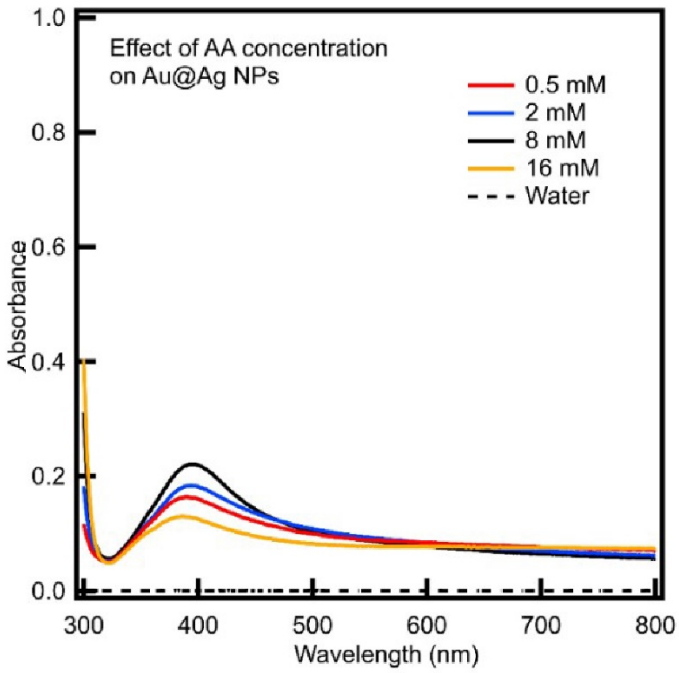

Figure S7. UV-vis spectra of Au@Ag NPs synthesized in separate batches using Au NP seeds, with concentrations of ascorbic acid ranging from 0.5 mM to 16 mM. The concentration of $AgNO_3$ (0.062 mM) and the volume % of Au NPs in the final solution (5%) is constant for all batches.

A broad plasmonic peak is observed in all spectra at a wavelength of 397 nm. Plasmonic peaks close to 400 nm are typically associated with Ag NPs[8] or with Au@Ag NPs rich in Ag.[9,10] Deconvoluting the spectra (Supplemental Section S5) also shows the presence of a secondary shoulder peak in all spectra at a wavelength close to 450 nm that may be associated with other multicomponent species such as Au@Ag NPs or Au-Ag nanoalloys rich in Au.[10,11] Additional studies are performed to determine the nature of species associated with both peaks in the UV-vis spectrum as described in Section S5.2.

S5.3. Identifying nature of species in seeded Au@Ag NP synthesis

For the seeded batch synthesis of Au@Ag NPs, the UV-vis spectra (Figure S7) are de-convoluted by fitting in IGOR Pro 8 into two Gaussian peaks: a primary peak (peak 0) and a secondary peak (peak 1). An example of a deconvoluted spectrum is shown in Figure S8.

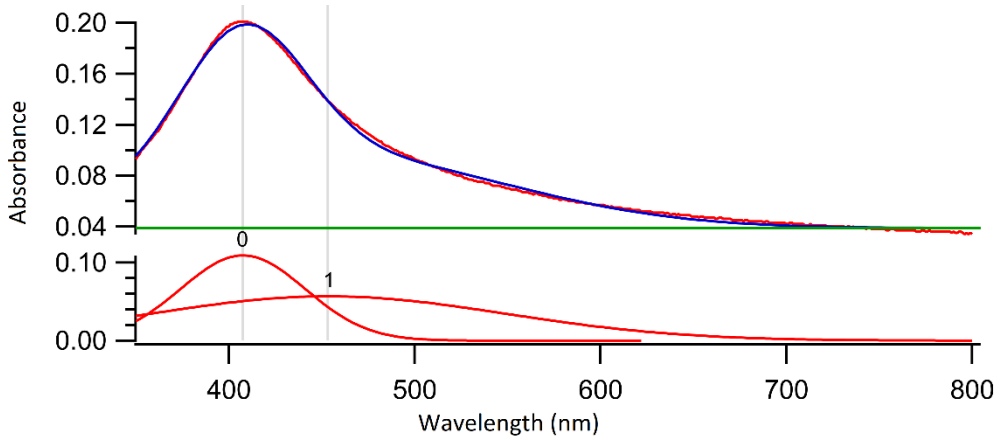

Figure S8. UV-vis spectra of a representative sample of seeded Au@Ag NPs synthesized using 8 mM ascorbic acid plotted in IGOR Pro 8: original spectrum *(top, red)*; fitted spectrum *(top, blue)*; and de-convoluted spectrum *(bottom, red)* showing a primary peak *(peak 0)* and a secondary peak *(peak 1)*. The concentration of $AgNO_3$ is 0.062 mM and the volume % of Au NPs in the final solution is 5%.

To identify the nature of the species associated with both peaks, initially the effect of $AgNO_3$ concentration on the UV-vis spectra of Au@Ag NPs is studied. The concentration of $AgNO_3$ in the seeded batch synthesis is varied from 0.016 mM to 0.496 mM in separate batches while maintaining the concentration of ascorbic acid (AA) at 8 mM and the volume % of Au NPs in the final product at 5%. The Au NPs are pre-synthesized in batch using 0.90 mM $NaBH_4$ and 0.27 mM $HAuCl_4$. The UV-vis spectra obtained for the seeded batches are shown in Figure S9 and the parameters of the de-convoluted UV-vis spectra are shown in Table S3.

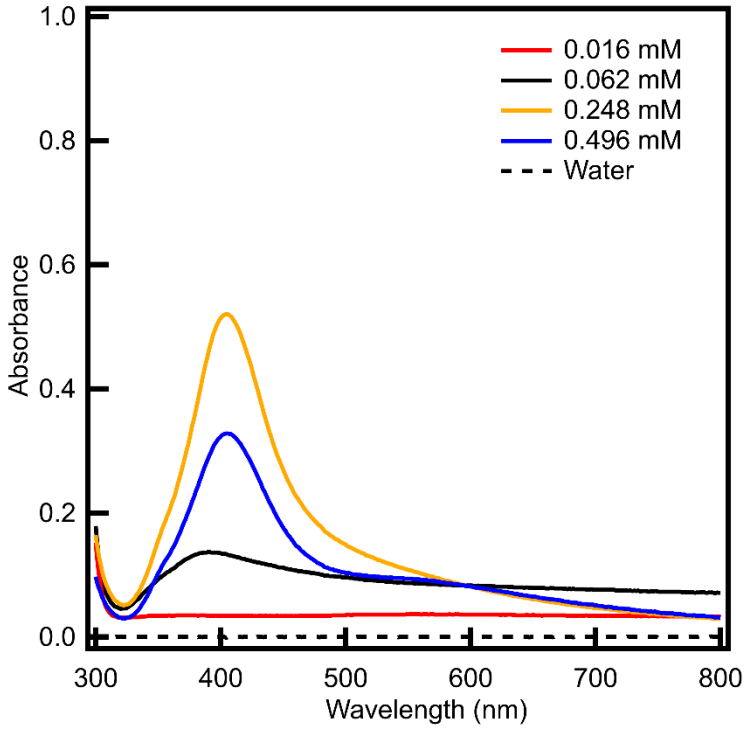

Figure S9. UV-vis spectra of Au@Ag NPs synthesized via seeded synthesis in separate batches with concentrations of $AgNO_3$ varying from 0.016 mM to 0.496 mM. Other reagent concentrations for all syntheses are: 8 mM AA and 5% by volume Au NPs in product solution. Au NP seeds are pre-synthesized using 0.27 mM $HAuCl_4$ and 0.90 mM $NaBH_4$ in batch at 200 RPM.

Table S3. Parameters (wavelength and absorbance) obtained from de-convoluted UV-vis spectra of seeded Au@Ag NPs synthesized in separate batches with concentrations of $AgNO_3$ varying between 0.016 mM to 0.496 mM. Each spectrum is de-convoluted into a primary Gaussian peak (Peak 0) and secondary Gaussian peak (Peak 1) using IGOR Pro 8. Other reagent concentrations for all syntheses are: 8 mM AA and 5% by volume Au NPs in product solution. Au NP seeds are pre-synthesized using 0.27 mM $HAuCl_4$ and 0.90 mM $NaBH_4$ in batch at 200 RPM.

$AgNO_3$ concentration (mM)	Peak 0		Peak 1		Peak 0/Peak 1 absorbance ratio
	Wavelength (nm)	Absorbance	Wavelength (nm)	Absorbance	
0.016*	-	-	-	-	-
0.062	396	0.055	487	0.025	2.2
0.248	405	0.876	469	0.256	3.4
0.496	408	1.789	495	0.436	4.1

*The synthesis with 0.016 mM $AgNO_3$ resulted in no plasmonic spectrum

It is observed from Figure S9 that all batches except the synthesis with 0.016 mM $AgNO_3$ result in plasmonic peak around 400 nm with a secondary peak at a higher wavelength. The absorbance of the primary peak increases with an increase in $AgNO_3$ concentration. These observations are corroborated by the parameters of the deconvoluted peaks shown in Table S3. Peak 0 for all batches has a wavelength close to 400 nm, suggesting the presence of either Ag NPs[8] or Ag-rich composites.[9,10] Peak 1 for all batches has a wavelength closer to 500 nm, suggesting the presence of either Au NPs or Au-rich composites.[1] The absorbance for both peaks increases with an increase in the $AgNO_3$ concentration, suggesting that the species associated with both peaks contain Ag and eliminating Au NPs as the source of Peak 1.

Mixing $AgNO_3$ with AA in batch at comparable reagent concentrations to the nanomaterial synthesis does not result in Ag NP formation via homogeneous nucleation, as suggested by Figure S5. However, the addition of Au NPs in the synthesis results in a plasmonic UV-vis spectrum as shown in Figure S9. Additionally, the absorbance of Peak 0 increases with an increase in $AgNO_3$ concentration, suggesting increased $AgNO_3$ reduction. These results suggest that only heterogeneous nucleation of Ag occurs on Au NPs at the reagent concentrations used.

The results (Figure S9 and Table S3) suggest that the two peaks are associated with Au-Ag bimetallic species. The absorbance of the peak at 397 nm can be directly related to the concentration of Ag-dominant bimetallic that is expected to form because of the high Ag:Au molar ratio of 4.6 in solution. The absorbance increases with an increase in the AA concentration up to 8 mM, after which it decreases at 16 mM AA (Figure S7). This observation supports the hypothesis that the rate of heterogeneous nucleation to form Au@Ag NPs increases with an increase in AA concentration. The further decrease in absorbance with an increase in AA concentration may be related to an excessive ion concentration in the solution. An increase in ionic concentration has

been previously associated with particle aggregation and coalescence.[12,13] The decrease in particle concentration resulting from aggregation may cause the decrease in absorbance. As the absorbance is highest at an AA concentration of 8 mM, this concentration is selected for the synthesis of Au@Ag NPs.

S5.4. Jet-mixing synthesis of seeded Au@Ag NPs without BSA

Subsequently, a standard batch synthesis is performed with the finalized reagent concentrations and analyzed by TEM to confirm Ag capping. A representative TEM image of Au@Ag NPs synthesized by seeded batch is shown in Figure S10a. The increase in particle size compared to that of Au NPs synthesized in batch (Figure S4) and the absence of small particles suggests the formation of a core-shell morphology.

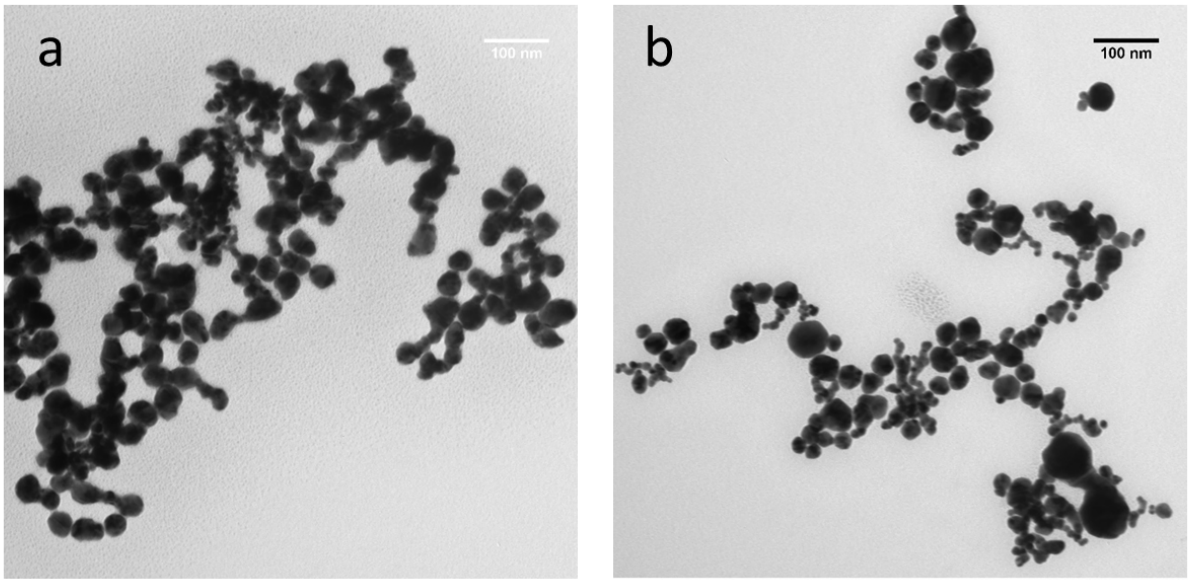

Figure S10. Representative TEM images of Au@Ag NPs synthesized in: a) batch and b) using single jet-mixing with Au NPs as seeds. Both syntheses are performed using the following reagent concentrations: 0.062 mM $AgNO_3$, 8 mM AA, and 5% by volume Au NPs in product. The main line and jet line flowrates in the single jet-mixer are 48 mL/h. Au NP seeds are synthesized using 0.27 mM $HAuCl_4$ and 0.90 mM $NaBH_4$ in batch at 200 RPM. These syntheses are performed in the absence of BSA as a stabilizing ligand.

The batch synthesis of seeded Au@Ag NPs is then translated to jet-mixing. The single jet-mixing assembly is used for synthesis at flowrates of 48 mL/h in the main line and jet lines with reagent concentrations comparable to the seeded batch synthesis. The product collected from the jet-mixing run is analyzed by UV-vis and its spectrum compared to that of the batch-synthesized counterpart. The UV-vis spectra for materials obtained from both processes are shown in Figure S11.

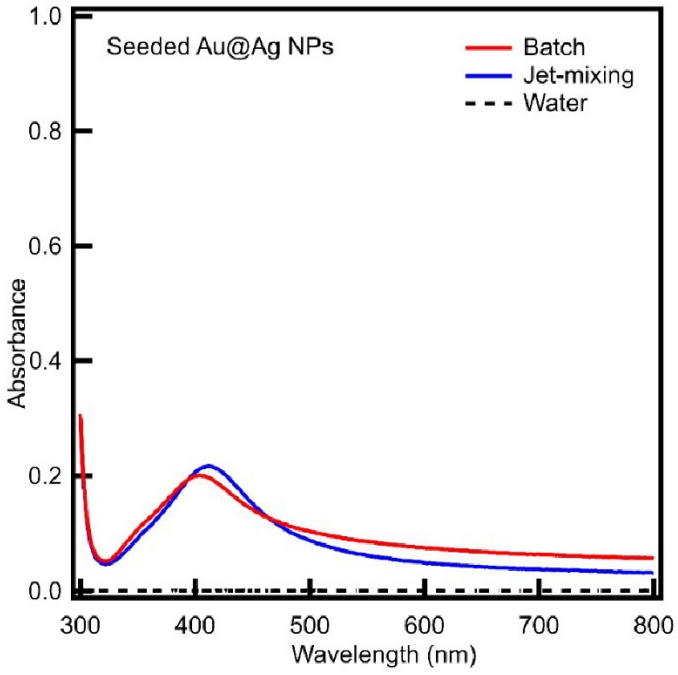

Figure S11. UV-vis spectra of seeded Au@Ag NPs obtained from batch *(red)* and single jet-mixing *(blue)* syntheses. Both syntheses are performed using the following reagent concentrations: 0.062 mM $AgNO_3$, 8 mM AA, and 5% by volume Au NPs in product. The main line and jet line flowrates in the single jet-mixer are 48 mL/h. Au NP seeds are synthesized using 0.27 mM $HAuCl_4$ and 0.90 mM $NaBH_4$ in batch at 200 RPM.

The spectrum of the batch-synthesized product has a broad peak with a maximum absorbance wavelength of 404 nm, and a similar peak is observed in the jet-mixing synthesized product at 412 nm. Deconvolution of the jet-mixing synthesized spectrum shows the presence of a secondary peak, as is observed in the Au@Ag NP seeded batch synthesis. The secondary peak wavelength is 455 nm for the batch-synthesized material and 436 nm for the jet-mixing synthesized material. The presence of two peaks suggests the formation of two bimetallic species: Ag-rich species indicated by the lower wavelength and Au-rich species indicated by the higher wavelength. The absorbance of the primary peak for the batch and jet-mixing synthesized materials is 0.092 and 0.118, respectively. The absorbance for the secondary peak is smaller, at 0.050 and 0.062, respectively. The higher absorbance for the primary peak suggests that Ag-rich bimetallic nanoparticles are dominant in both materials, assuming the extinction coefficients for both bimetallic species are comparable. Overall, these results suggest that the plasmonic properties of seeded Au@Ag NPs obtained from both processes are comparable. These observations support our hypothesis that the rate of heterogeneous nucleation contributing to Au@Ag NP formation is promoted by: (1) decreasing $NaBH_4$ concentration in Au NP synthesis from 2.40 mM to 0.90 mM; and (2) increasing AA concentration in seeded Au@Ag NP synthesis from 2 mM to 8 mM.

Next, the single jet-mixing synthesized Au@Ag NPs are analyzed by TEM. A representative TEM image is shown in Figure S10b. There is an increase in particle size compared to the Au NPs seeds (Figure S4), suggesting the formation of a core-shell morphology. The particle size obtained from the modified seeded jet-mixing synthesis is comparable to its batch counterpart. The average size and standard deviation obtained for the primary size distribution (particles > 15

nm) in the jet-mixing synthesized material (31±7 nm, 23% s.d.) is comparable to that obtained for the batch-synthesized material (33±8 nm, 24% s.d.). A small concentration of secondary particles is obtained in the jet-mixing synthesized material as observed in the TEM images, which requires further investigation. However, these observations suggest that the size distribution of Au@Ag NPs obtained through jet-mixing can be tuned such that it is comparable to that obtained from the batch-synthesized counterpart by optimizing process parameters for the jet-mixing system. Overall, these studies demonstrate that the process of Ag shell formation on Au NP seeds during Au@Ag NP synthesis can be translated from batch to a continuous process while retaining key properties of the nanomaterials synthesized at the lab-scale.

S6. Composition analysis of core@shell nanoparticles.

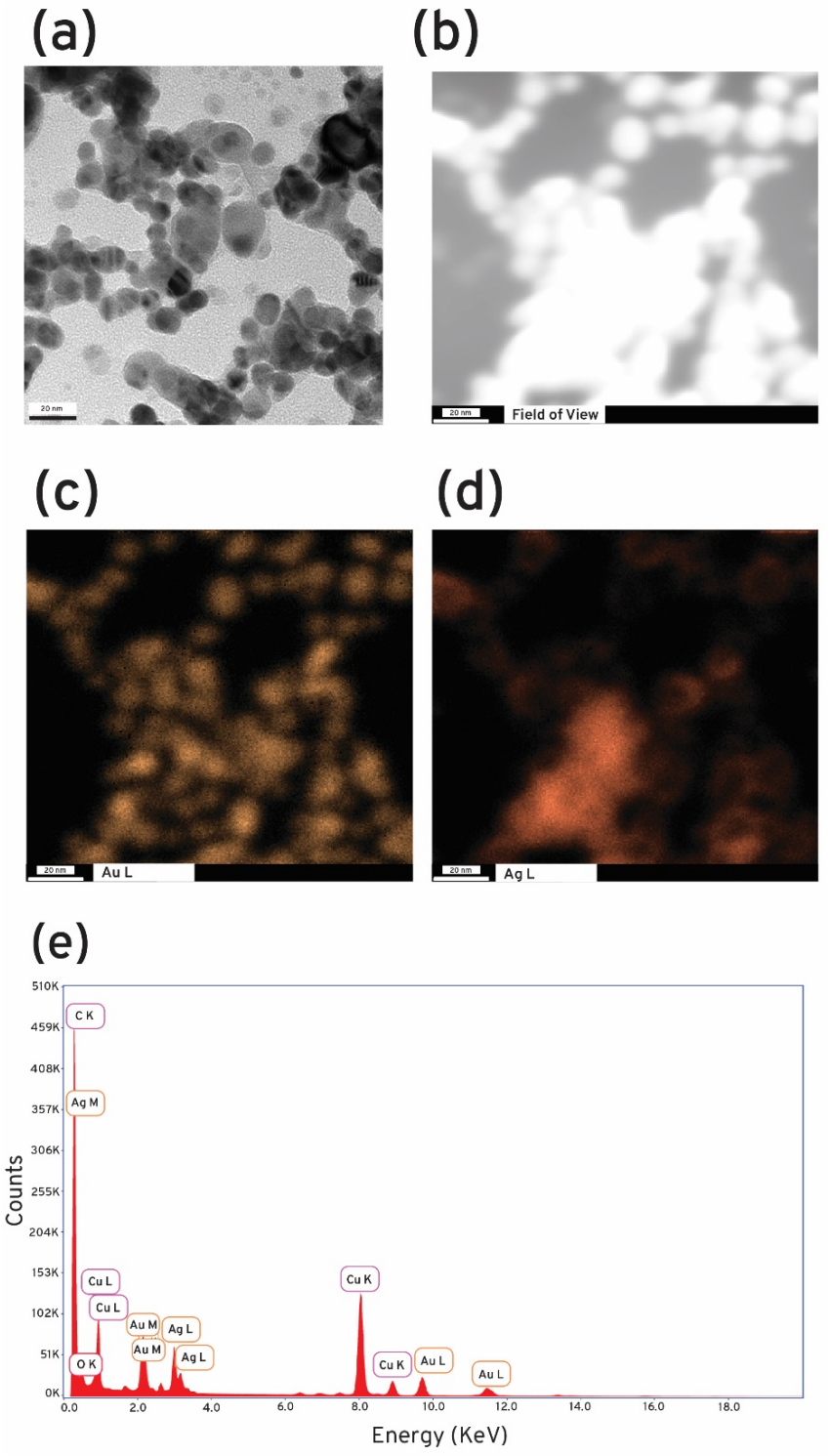

Figure S12. (a) TEM imaging of Au@Ag nanocomposites, (b) Field of view for EDX mapping, (c) Au mapping, (d) Ag mapping, and (e) EDX spectrum across the field of view.

References:

1. Deraedt, C. *et al.* Sodium borohydride stabilizes very active gold nanoparticle catalysts. *Chem. Commun.* **50**, 14194–14196 (2014).
2. Wagner, J. & Köhler, J. M. Continuous synthesis of gold nanoparticles in a microreactor. *Nano Lett.* **5**, 685–691 (2005).
3. Huang, H. *et al.* Continuous flow synthesis of ultrasmall gold nanoparticles in a microreactor using trisodium citrate and their SERS performance. *Chem. Eng. Sci.* **189**, 422–430 (2018).
4. Thanh, N. T. K., Maclean, N. & Mahiddine, S. Mechanisms of nucleation and growth of nanoparticles in solution. *Chem. Rev.* **114**, 7610–7630 (2014).
5. Parulkar, A. & Brunelli, N. A. High-Yield Synthesis of ZIF-8 Nanoparticles Using Stoichiometric Reactants in a Jet-Mixing Reactor. *Ind. Eng. Chem. Res.* **56**, 10384–10392 (2017).
6. Liu, X., Atwater, M., Wang, J. & Huo, Q. Extinction coefficient of gold nanoparticles with different sizes and different capping ligands. *Colloids Surfaces B Biointerfaces* **58**, 3–7 (2007).
7. Shin, Y. *et al.* Microfluidic Multi-Scale Homogeneous Mixing with Uniform Residence Time Distribution for Rapid Production of Various Metal Core–Shell Nanoparticles. *Adv. Funct. Mater.* **2007856**, 1–10 (2020).
8. Agnihotri, S., Mukherji, S. & Mukherji, S. Size-controlled silver nanoparticles synthesized over the range 5–100 nm using the same protocol and their antibacterial efficacy. *RSC Adv.* **4**, 3974–3983 (2014).
9. Rodríguez-González, B., Burrows, A., Watanabe, M., Kiely, C. J. & Marzán, L. M. L. Multishell bimetallic AuAg nanoparticles: Synthesis, structure and optical properties. *J. Mater. Chem.* **15**, 1755–1759 (2005).
10. Knauer, A., Eisenhardt, A., Krischok, S. & Koehler, J. M. Nanometer precise adjustment of the silver shell thickness during automated Au-Ag core-shell nanoparticle synthesis in micro fluid segment sequences. *Nanoscale* **6**, 5230–5238 (2014).
11. Herbani, Y., Nakamura, T. & Sato, S. Synthesis of near-monodispersed Au-Ag nanoalloys by high intensity laser irradiation of metal ions in hexane. *J. Phys. Chem. C* **115**, 21592–21598 (2011).
12. French, R. A., Jacobson, A. R., Kim, B., Isley, S. L. & Penn, R. L. E. E. Influence of Ionic Strength , pH , and Cation Valence on Aggregation Kinetics of Titanium Dioxide Nanoparticles. *Environ. Sci. Technol.* **43**, 1354–1359 (2009).
13. Ranadive, P., Parulkar, A. & Brunelli, N. A. Jet-Mixing for the Production of Monodisperse Silver Nanoparticles Using Reduced Amounts of Capping Agent. *React. Chem. Eng.* **4**, 1779–1789 (2019).